Structural analysis of pure and zinc doped Bismuth Ferrite by Spray pyrolysis method

Tapan Kumar pani[1], Bibekananda Sundaray[1] and Dibyaranjan Rout[2]

[1]Department of Physics,Ravenshaw University, Cuttack -753003,India

tapanpani70@gmail.com, bnsundaray@gmail.com

[2]Kalinga Institute of Industrial Technology, Bhubaneswar-751024, India

Abstract-Multiferroic $BiFe_{(1-x)}Zn_xO_3$ (x=0.00,0.03) thin films were prepared on glass substrates by using spray pyrolysis method. The prepared samples sintered at different temperature for 2h show a single phase nature. The structural properties were investigated using XRD and FESEM.. X-ray diffraction studies indicates distorted rhombohedral R3c perovskite structure FESEM images shows the change of grain size from nearly spherical to elongated shape with Zn substitution. The structural change might be an important factor for achieving the ferroelectric properties in these materials.

Keywords: Bismuth Ferrite, Multiferroics, Spray pyrolysis, Thin films

1 Introduction

Research on multiferroic materials has become most popular in recent years because these materials have two or more types of ferroic properties, such as ferromagnetism, ferroelectricity and ferroelasticity in the same phase due to their attractive dielectric properties. The specific features of the perovskite structure, especially concerning its chemical and structural versatility (the substitution of various cations, the distortions of the perovskite crystal lattice and the formation of defects take place smoothly), admit to fabricate a wide variety of materials [1]. Complex perovskite materials $A(BB')O_3$ and $AA'(BB')O_3$, are widely used in various electronic and microelectronic functional devices such as capacitors dielectrics, microwave frequency resonators, semiconducting thermistors , sensors, electrode materials, actuators spintronic devices etc. on the field of multiferroic application.

In multiferroic materials, $BiFeO_3$ (BFO) is the material that shows both anti-ferromagnetic and ferroelectric properties at room temperature. Its ferroelectric Curie temperature (Tc~1103 K) and anti-ferromagnetic Neel temperature (T_N~643 K) are high above the room temperature [2, 3]. In comparison with bulk ceramic BFO, BFO thin films have more theoretical remnant polarization (Pr~100 mC/cm^2) [4, 5], which makes it possible to be used in the future-generation ferroelectric memories. However, BFO films usually have high leakage current density, because of the existence of oxygen vacancies and various oxidation states of Fe ion (Fe^{3+} to Fe^{2+}state) [5]. Therefore it is required to decreasing the leakage current density. At present work, the performance of BFO film is optimized by improving the preparation process and ion doping.

The formation of defect complexes between cationic acceptors and oxygen vacancies plays a major role in the improvements of electrical and ferroelectric properties of the Ti and Zn doped BFO thin film. In particular, the Zn doping was found to improve the magnetic properties and electrical properties of the films. Significant saturation magnetization enhancement has been observed in Zn-doped BFO by Liu et al. [6]. Han et al .observed that Mn and Zn co-doping could result in a large remnant magnetization (Mr) of 0.045emu/g [7].

2 Experimental Details

$BiFe_{1-x}Zn_xO_3$ (x=0.00,0.03) multiferroic thin films were prepared by a spray pyrolysis method. Bismuth nitrate ($Bi(NO_3)_3{\cdot}5H_2O$), iron nitrate ($Fe(NO_3)_3{\cdot}9H_2O$), and zinc nitrate ($Zn(NO_3)_2{\cdot}6H_2O$) were purchased from Himedia laboratories, India and used without any further purification. According to the molecular formula $BiFe_{1-x}Zn_xO_3$, proper amounts of the initial reactants are taken in stoichiometric ratio. Bismuth nitrate ($Bi(NO_3)_3{\cdot}5H_2O$), iron nitrate ($Fe(NO_3)_3{\cdot}9H_2O$), and zinc nitrate ($Zn(NO_3)_2{\cdot}6H_2O$), were dissolved in 50 mL ethylene glycol solution with a concentration of 0.5 mol/L. To compensate the bismuth loss 10%excess of bismuth nitrate will taken. The thin film of BFO is deposited on a pre-cleaned glass slide pieces by spraying precursor solution using Holmarc opto-mechatronics spray pyrolysis equipments at 450^0C. The samples were sintered at temperature 500^0C and 550^0C for 2h using muffle furnace in air atmosphere. The structural characterization and phase identification of the samples were performed by using X-ray diffraction (Rigaku Ultima IV X-ray Diffractometer , Japan).The reitveld analysis of the XRD data was analysed by Fullprof software. The energy-dispersive spectroscopy (EDS) pattern and morphology of the samples were examined with scanning electron microscopy (SEM Zeiss Supra 55).

3 Results and Discussions-

Fig. 1 shows X-ray diffraction (XRD) patterns of the pure BFO and the Zn doped BFO thin films deposited on glass substrates. The crystal structure of the sintered sample is examined by an X-ray diffraction (Rigaku Ultima IV X-ray Diffractometer). CuK_α radiation (λ = 1.5406 Å). The data is analyzed by the Rietveld method using the ''Fullprof'' software to assess phase purity and the crystal structures of the material. The Bragg peaks are modeled with pseudo-Voigt function and the background is estimated by linear interpolation between selected background points. The complete data of reitveld analysis is shown in table-1.The analyses of the XRD pattern confirm a single phase formation without any impurity phase in all thin films, which shows the proper preparation of the solution and the process of heat treatment at the time of preparation and sintering. The rhombohedral distorted perovskite structure of $BiFeO_3$ with R3c space group is conserved. All the peaks of the undoped sample (x = 0.00) were indexed to rhombohedrally distorted perovskite structure with R3c space group which are well matched with the JCPDS Card no: 72-2035. The formations of the pure perovskite phases were confirmed by the absence of additional peaks corresponding to the impurity phases in both the films. However, as shown in Figs. 1(b) and 1(c) small changes in the diffraction in the BFZO thin film and this shift is not significant to change the original

perovskite structure. These results indicate that the internal stress induced by the Zn elements leads to the distortion in perovskite without changing the original structure. Additionally, the presence of these impurity phases may be arrived due to the volatile nature of Bi and the high sensitivity of the Fe atoms at high sintering temperatures. The shifts in the diffraction peaks may be caused by the difference in ionic radius between Fe^{3+} (R_{Fe} = 0.65 Å) and Zn^{2+} (R_{Zn} = 0.74 Å) [8].

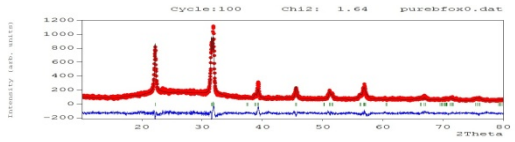

(a)

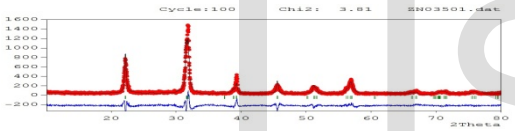

(b)

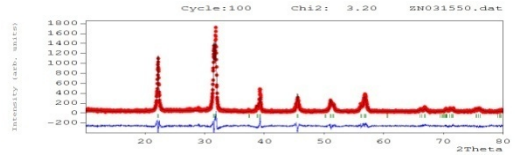

(c)

Fig-1: Rietveld refinement of (a) Pure BFO film(b) Zn doped BFO film sintered at 500^{0}C (c) Zn doped BFO film sintered at 550^{0}C

The typical micro structural features were analyzed by examining the FESEM micrographs and EDX patterns of BFO and doped $BiFe_{0.97}Zn_{0.03}O_3$ thin films are shown in Fig. 2, 3 and 4 respectively. The lines of Fe, O, Bi, and Zn are studied in the EDX patterns of the doped samples. The SEM micrographs reveal a microstructure comprising grains of varying shapes with diameters below 20μm reduced diameter of approximately 10 μm.

Table-1: Details of Rietveld refinement of structural parameters of BFO and BFZO thin film.

	Pure BFO	Zn doped BFO ($BiFe_{0.97}Zn_{0.03}O_3$)	
Sintering Temp.	550^{0}C	550^{0}C	500^{0}C
Space Group	R3c	R3c	R3c
a(Å)	5.582354	5.577255	5.573713
b(Å)	5.582354	5.577255	5.573713
c(Å)	13.867468	13.850354	13.828204
α	90^0	90^0	90^0
β	90^0	90^0	90^0
γ	120^0	120^0	120^0
χ2	1.64	3.20	3.81
Rp(%)	53.9	37.1	45.6
Rw(%)	38.0	35.6	41.6
Rexp(%)	29.69	19.90	21.33
Over all B-factor	5.6078	3.4130	3.7835
RF Factor	17.38	11.39	11.91
Bragg R-factor	12.98	8.373	9.605
U	0.137962	1.294917	0.470980
V	-0.007618	-0.007618	-0.007618
W	0.168607	1.184871	0.360856
IG	-0.117341	-1.149792	-0.295264
Scale	0.20604×10^{-5}	0.33303×10^{-5}	0.2975×10^{-5}

. In the un-doped BFO thin films the Spherical grains with diameters of approximately 10 μm were observed. In contrast, with doping of Zn ion (x = 0.03) the grain morphology changed to a elongated shape with a remarkably It can observed that this morphological changes in the BFO concentration for the low value of x, the Zn concentration had only a slightly change on the morphology of the grains. However, the BFO thin film became elongated when the Zn concentration was increased. The nucleation rate of the grains are supposed to be change much more when the Zn concentration exceeded a certain limit and this would have noticed in a different grain morphology compared with that of the un-doped and less-doped BFO. Interestingly, the average grain size of the un-doped BFO film was larger than that of the doped samples. The grain sizes of the films decreased with increasing Zn concentration, which may be due to the difference in the ionic radius of Fe^{3+} and Zn^{2+}. The substitution of larger Zn^{2+} ions at Fe-sites filled the empty space completely, which further suppressed grain growth and led to a smaller grain size. This is in good agreement with the XRD results discussed above. There is another fact about the reduction in grain size i.e. Zn^{2+} acquired a lower valence state than Fe^{3+}. Therefore, the presence of Zn^{2+} may have controlled the reduction of Fe^{3+}, which would affect the grain growth and give rise to a small grain size in the system. .

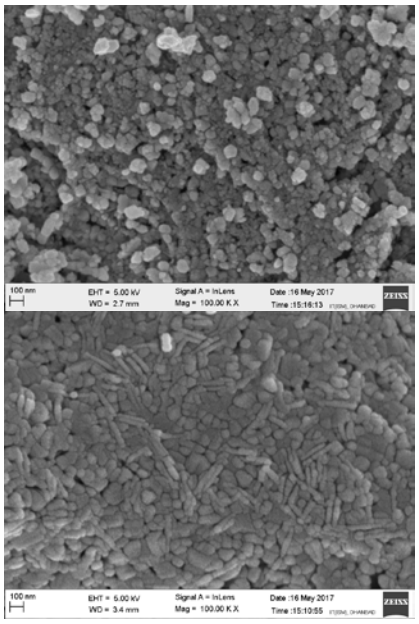

(Fig-2: FESEM of pure BFO and Zn doped BFO)

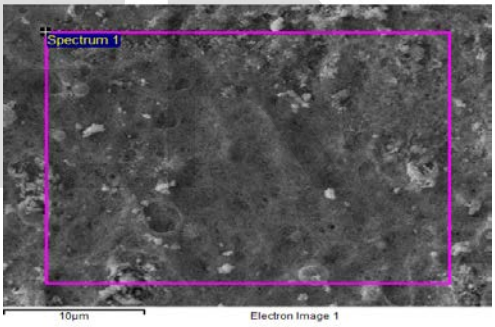

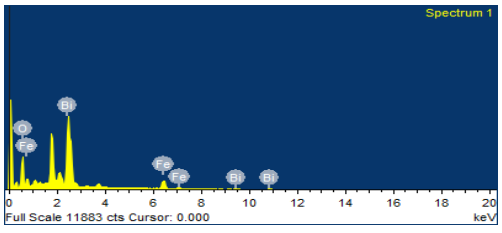

(Fig-3: EDX of pure BFO)

Fig. 3 and 4 shows the EDAX analysis of pure and Zinc doped BFO (x = 0.03) thin films and it explain the quantitative studies of the various constituent elements present in the sample. It has

been observed that the percentage content of the constituting elements as given by EDAX studies and empirical formula were comparable to each other. Hence, EDAX studies predicted the chemical purity as well as the required proportion of the constituents in all the thin film.

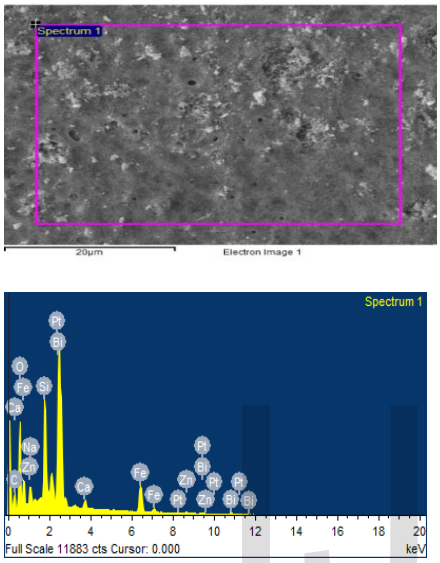

(Fig-4: EDX of Zinc Doped BFO)

4 Conclusions

In summary, comparative studies were made on the pure $BiFeO_3$ (BFO) and the Zn doped (BFZO) thin films prepared by the spray pyrolysis method. Their structures were analyzed by XRD, FESEM and EDX. The XRD results confirm that all samples possess a rhombohedral perovskite structure with the R3c space group, and no structural transition occurred upon Zn doping. FESEM analysis indicated that the substitution of Fe with Zn suppressed the grain growth and slightly decreased the grain size of the material.

Acknowledgments-

One of the authors TKP acknowledges the project fellowship from SERB, New Delhi. The authors acknowledge Department of Geology, Ravenshaw University, Cuttack for providing XRD facilities.

References

[1] A.S. Bhalla, R. Guo, R. Roy, The perovskite structure-a review of its role in ceramic science and technology, J. Mat. Res. Innovat 4 (2000) 3.

[2] J. Wang, J.B. Neaton, H. Zheng, V. Nagarajan, S.B. Ogale, B. Liu, D. Viehland, V. Vaithyanathan, D.G. Schlom, U.V. Waghmare, N.A. Spaldin, K.M. Rabe, M. Wutting, R. Ramesh, Epitaxial BiFeO3 multiferroic, Science 299 (2003) 1719e1722.

[3] C. Ponzoni, R. Rosa, M. Cannio, V. Buscaglia, E. Finocchio, C. Leonelli, Optimization of BFO microwave-hydrothermal synthesis: influence of process parameters,J. Alloy. Compd. 558 (2013) 150e159.

[4] J.J. Xie, C.D. Feng, X.H. Pan, Y. Liu, Structure analysis and multiferroic properties of Zr4+ doped BiFeO3 ceramics, Ceram. Inter. 40 (2014) 703e706.

[5] R.Y. Zheng, C.H. Sim, J. Wang, S. Ramakrishna, Effects of SRO buffer layer on multiferroic BiFeO3 thin films, J. Am. Ceram. Soc. 91 (10) (2008) 3240e3244.

[6] J. Liu, H.M. Deng, X.Z. Zhai, T. Lin, X.J. Meng, Y.Y. Zhang, W.L. Zhou, P.X. Yang, J.H. Chu, Influence of Zn doping on structural, optical and magnetic properties, of BiFeO3 films fabricated by the sol-gel technique, Mater. Lett. 133 (2014) 49e52.

[7] Y.M. Han, Y.H. Ma, C.Y. Quan, N. Gao, Q.X. Zhang, W.W. Mao, J. Zhang, J.P. Yang, X.A. Li, W. Huang, Substitution-driven structural, optical and magnetic transformation of Mn, Zn doped BiFeO3, Ceram. Inter. 41 (2015) 2476e2483.

[8] L.H. Ahrens, The use of ionization potentials Part 1. Ionic radii of the elements, Geochimica et cosmochimica Acta, 2 (1952) 155-169.